Russell, B. K., Takeda, S., Ward, C., & Hamerton, I. (2019). Examining the influence of carboxylic anhydride structures on the reaction kinetics and processing characteristics of an epoxy resin for wind turbine applications. *Reactive and Functional Polymers*, *144*, [104353]. https://doi.org/10.1016/j.reactfunctpolym.2019.104353

Examining the influence of carboxylic anhydride structures on the reaction kinetics and processing characteristics of an epoxy resin for wind turbine applications.

Bethany Russell[1,], Shinji Takeda[2], Carwyn Ward[1], Ian Hamerton[1]*

[1] Bristol Composites Institute (ACCIS), Department of Aerospace Engineering, Queen's Building, University of Bristol, University Walk, Bristol, BS8 1TR, U.K.

[2] Hitachi Chemical Co. Ltd., Tokyo, Japan.

* *Correspondence: beth.russell@bristol.ac.uk*

Abstract

The cure of a low molecular weight (approximate EEW = 184 g/mol), difunctional epoxy resin based on bisphenol A has been studied in the presence of three carboxylic anhydrides: 3- or 4-methyl-1,2,3,6-tetrahydrophthalic anhydride, 3- or 4-methyl-hexahydrophthalic anhydride, and methyl3,6-endomethylene-1,2,3,6-tetrahydrophthalic anhydride, and a tertiary amine (Ancamine K54). The formulated blends display complex viscosities ranging from 36 to 58 mPa.s and at 75 °C, the blends take between 56 and 73 minutes to reach gelation, with the highest viscosity and

longest gel time observed for the blend containing methyl-3,6-endomethylene-1,2,3,6-tetrahydrophthalic anhydride. Rate constants of 6.8 to 14 s^{-1} at 75 °C and activation energies of 69 to 78 kJ/mol are determined using dynamic differential scanning calorimetry. Glass transition temperatures for the cured blends are similar, at 100 °C, with conversions of 83 to 89% observed. The cured blend containing methyl-3,6-endomethylene-1,2,3,6-tetrahydrophthalic anhydride displays the poorest thermal stability in terms of the onset of degradation, while yielding the highest char yield of the blends studied.

KEYWORDS: wind turbines; epoxy resins; anhydrides; rheology, thermal analysis; kinetics.

1 Introduction

The wind turbine industry has been using composite materials for wind turbine blades since the 1970s [1] , due to their ability to offer high rigidity and strength whilst minimising weight. Owing to the increased demand for renewable energy sources, the desire to build larger and more efficient wind turbines is growing. Where current composite materials meet the specific requirements for 80 m turbine blades, the industry is now looking to make larger blades (*e.g.* GE's proposed Haliade-X blade which will have a blade length of 107 m [2]) to meet growing demands for green energy [1]. With increasing size, gravitational forces and inertial loads tend to dominate over aerodynamic loads, thus creating more design challenges. To reduce the weight of these larger turbine blades, the industry is looking towards carbon fibre composite systems [3].

With this trend, there is increased industrial focus on developing improved polymer matrix systems, which have been designed specifically for this application. Currently, the method employed most widely for the manufacture of wind turbine blades is resin infusion and it follows

that resins must have low viscosity at manufacturing temperatures and long processing windows to allow for such a large part to be infused [4,5]. Interfacial properties between the resin and fibres are critical to the performance of the part to improve the transfer of load between fibres and improve the composite interlaminar properties [6]. Furthermore, wind turbine blades are intended to have service lives of 20-30 years, while exposed to harsh conditions and with little maintenance, thus any material developments which can improve their performance and minimise downtime are of great interest to the industry [7].

Owing to their compatibility with glass fibres, polyester resins were previously widely used in wind turbine blade applications, but in recent years they have been superseded by epoxy resins, which exhibit superior mechanical performance and improved fatigue resistance. Epoxy resins are one of the most mature thermosetting resin families [8], with an established heritage in advanced composite applications dating back some 50 years and have been widely reported in literature. The versatility of epoxy resins arises from their ability to undergo cure with a wide variety of compounds, including polyamines, thiols, imidazoles [8,9], and more recently ionic liquids [10]. This work will focus upon tertiary amine-catalysed anhydride-cured epoxies, for which a clear reaction mechanism is still under discussion [11,12]. In this work it is assumed the reaction proceeds in two main steps as the amine and anhydride are pre-reacted before the addition of the epoxy, for which a general reaction scheme is given in Fig. 1. The amine and anhydride are pre-reacted to form an anion, which can then react with the epoxy ring causing ring opening. The homopolymerisation reaction then propagates leading to the development of a highly crosslinked, three-dimensional network [11,12]. The effects of the curing agent stoichiometry on crosslink density have been well established for amine-cured epoxy resin systems [13,14], although there

are fewer studies on anhydride-cured epoxy resins [8,15], it is known that this impacts upon the thermal and mechanical properties of the resin.

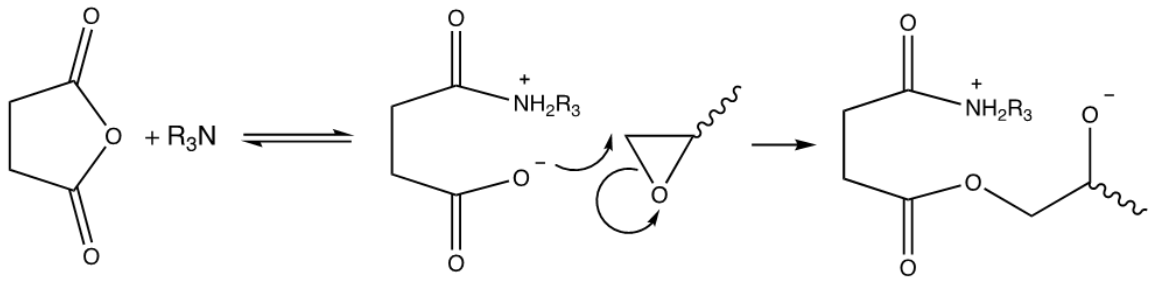

Fig. 1. Scheme showing mechanism of tertiary amine-catalysed epoxy-anhydride reaction.

Anhydride-cured epoxy resins have been exploited in recent decades as they have been shown to reduce the mix viscosity of the resulting epoxy formulations without the need for additional diluents which, in turn, makes them ideal curing agents for infusion processed epoxies [16]. It has also been reported that they experience lower chemical shrinkage than their diamine-cured counterparts and thus display reduced residual stresses within the resultant composite. Residual stresses often cause laminate defects such as warpage, delaminations, and cracks, which can compromise the overall performance [17].

We have previously reported the physical and mechanical properties of glass-reinforced polymer (GFRP) composites based on one of the blends (**1**) contained in the present work [18], for which improved interfacial properties have been observed. In the present study the cure characteristics of three related anhydrides will be evaluated, when used as the curing agent for a tertiary amine and bisphenol-A glycidyl ether epoxy resin system, to establish structure-property relationships. The aim is to show how these small differences in the anhydride structure may enhance the physical

and mechanical properties and allow for tailoring of the polymer network for specific wind turbine applications.

2 Experimental methods

2.1 Materials.

The diglycidyl ether of bisphenol A (DGEBA, A, approximate EEW = 184 g/mol) and anhydrides: 3- or 4-methyl-1,2,3,6-tetrahydrophthalic anhydride (C), 3- or 4-methyl-hexahydrophthalic anhydride (D), and methyl-3,6-endomethylene-1,2,3,6-tetrahydrophthalic anhydride (E) and tertiary amine (Ancamine K54) were supplied by Hitachi Chemical Co. Ltd., all monomer materials (Table 1) were used as received without further purification.

Table 1. The chemical structures of the monomers used in this work.

Chemical Name	Letter	Structure
bisphenol A diglycidyl ether (DGEBA) *N.B.* n = 0 - 1	**A**	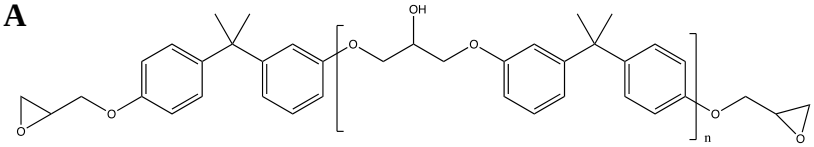
tris-2,4,6-(dimethylaminomethyl) phenol (90-95 wt%) and bis(dimethylaminomethyl) phenol (5-10 wt%) (Ancamine K54)	**B**	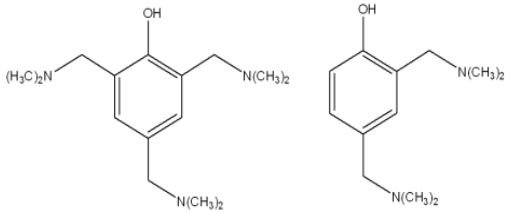
3- or 4-methyl-1,2,3,6tetrahydrophthalic anhydride (HN2200)	**C**	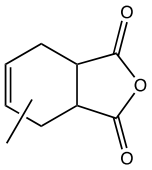
3- or 4-methylhexahydrophthalic anhydride (HN5500)	**D**	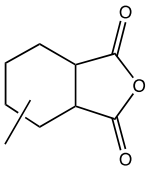
methyl-3,6endomethylene-1,2,3,6tetrahydrophthalic anhydride (MHAC-P)	**E**	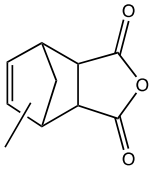

2.2 Formulation and curing of epoxy resin.

The blends were prepared by weighing the tertiary amine, **B** (2.63 wt%) with either of the anhydrides **C**, **D**, or **E** (44.74 wt%) into a 100 ml reaction vessel (without the lid, coated three times with a mould release agent) in the desired ratios and stirred by hand at room temperature until homogenised. The epoxy, **A** (52.63 wt%) was then added and stirred until homogenised. The resulting blend was poured into the desired mould, in which it was degassed for 15 minutes at room

temperature in a vacuum chamber until no further outgassing was observed. Resin samples were cured in a convection oven using the prescribed cure cycle: ramp to 75 °C at 2 °C/min and then dwell for 12 hours. The resulting blends will be referred to as **1**, **2**, and **3** as denoted in Table 2.

Table 2. The assignment of blend numbers indicated by the blend substituents

Blend constituents	Blend number
A, B, **C**	**1**
A, B, **D**	**2**
A, B, **E**	**3**

2.3 Analytical Measurements

2.3.1 Rheological analysis.

Rheology measurements were performed using a TA Discovery HR-1 hybrid rheometer instrument (TA Instruments) equipped with a parallel plate fixture. The disposable aluminium plates (25 mm in diameter with a gap of 0.3 mm) were used, due to the low viscosity of the systems measured. Isothermal experiments were conducted at 75 °C to assess the time taken to reach gelation and to monitor the changes in viscosity over the cure. The chamber was heated to 75 °C and equilibrated at this temperature for 10 minutes before the sample was loaded on to the plates. A strain frequency of 1 Hz and an oscillation amplitude of 1.5% were selected as the response was within the linear viscoelastic regime.

2.3.2 Dynamic scanning calorimetry (DSC).

DSC experiments were performed using a TA DSC Q2000 calorimeter. Hermetically sealed Tzero aluminium pans were used, with sample masses between 6-10 mg for both uncured and cured

samples. Samples were equilibrated at 30 °C and then heated to 250 °C at a heating rate of 10 °C/min, unless otherwise stated, with the sample cell kept under a constant nitrogen flow (50 cm^3/min). The presence of any residual curing exotherms was identified by modulated DSC (MDSC) thermograms, the temperature was swept from 25-250 °C with a ramp rate of 3 °C/min. The modulation period selected was 60 s with a modulation temperature amplitude of +/- 1 °C. The cure kinetics were studied *via* dynamic DSC of uncured resin using selected heating rates (5, 10, 15, and 20 °C/min) over the temperature range 25-250 °C.

2.3.3 Dynamic mechanical analysis (DMA).

DMA experiments were performed in tensile mode with a Mettler Toledo DMA/STDA 1+. Cured resin samples of cuboidal geometry: thickness 0.76 (+/- 0.1) mm; width 3.3 (+/- 0.1) mm; and gauge length 10.5 mm were machined. Samples were equilibrated at -50 °C before ramping at 5 °C/min to 170 °C. The displacement amplitude was 5 µm and frequency 1 Hz, with force 1 N and static (pre-tension) force of 1.5 N.

2.3.4 Fourier Transform Infrared (FTIR) Spectroscopy.

FTIR spectra were obtained in transmission mode for both the uncured and cured resins over the range 4000-600 cm^{-1} using a Perkin Elmer Spectrum 100 spectrometer. Four spectra were obtained at a resolution of 4 cm^{-1} and co-added to produce the final spectrum.

2.3.6 Simultaneous Thermal Analysis (STA).

STA data were acquired using a Netzsch STA 449 F5. Samples were weighed into aluminium crucibles (~18 mg), and using an autosampler, the crucibles were loaded into the furnace and

exposed to following temperature profile: equilibrated for 10 minutes at 25 °C, ramped at 10 °C/min to 800 °C, before cooling to room temperature. All experiments were conducted under flowing nitrogen (50 cm^3/min).

3 Results and discussion

3.1 Preparation and properties of cured blends.

The preparation of the three blends resulted in obvious differences in the appearance of the uncured and cured blends (see Supplementary Table S1). The most vibrantly coloured of these came from blend **1**, which is bright pink in its uncured state, due to the charge transfer complex formed from the mixing of the amine and anhydride (**C)**. On curing, a straw-coloured transparent plaque is formed.

3.2 Examining the processability of the blends.

The intended application of these resins is in the production of wind turbine blades, in which the principal manufacturing route involves vacuum assisted resin transfer moulding (VaRTM), a process which pulls uncured resin though a preform of dry fabric. The infusion process is affected by several factors including: the resin viscosity (which ideally falls below 500 cPs/0.5 Pa.s at the processing temperature) [5], fabric permeability, and the infusion strategy (number and location of resin inlets) chosen. Thus, understanding the relationship between the resin viscosity, gelation time, and polymerisation kinetics is necessary. The evolution of the complex viscosity was monitored for each of the three resin blends at the cure temperature (75 °C) and is given in Fig. 2 and Table 3. All three resin blends display similar initial viscosities, indicating that their infusion times should be comparable under these conditions. The time taken for the complex viscosity of

each blend to exceed 1 Pa.s is also similar (Table 3), regardless of anhydride structure, with variation of no more than 1 to 2 minutes. It should be noted that the infusion process is usually conducted at lower temperatures, typically at 50 °C and as all resins displayed similar initial viscosities at 75 °C it was assumed the same would hold true at lower temperatures. An isothermal experiment at 50 °C (processing temperature) was conducted for resin blend **1**, in which the complex viscosity remained below 0.5 Pa.s for 100 minutes. This indicated that all three resin blends have long processing windows making them suitable for infusion of large wind turbine blades.

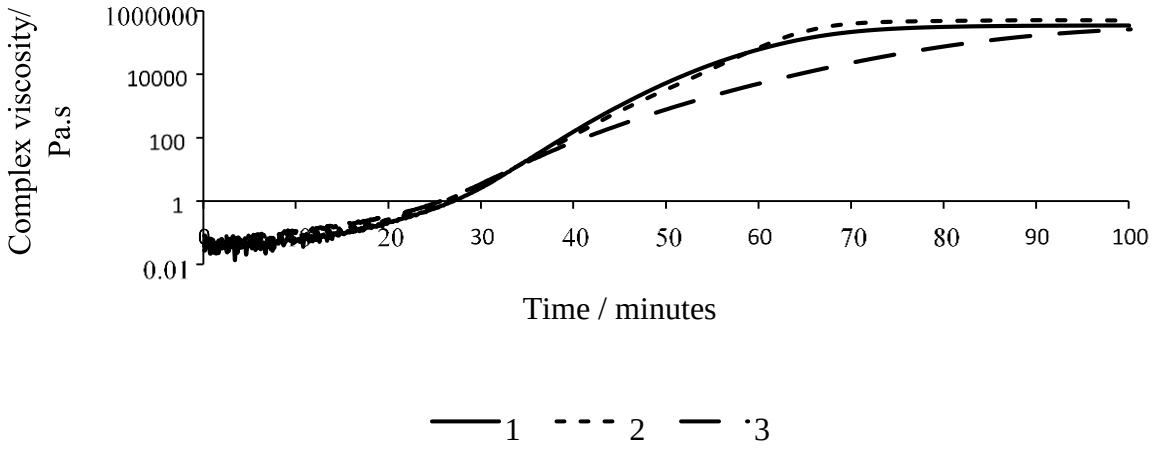

Figure 2. Complex viscosity data for each of the three resin blends, **1**, **2**, and **3** at 75 °C.

Table 3. Rheological behaviour measured at 75 °C for the blends studied in this work.

Blend	Initial complex viscosity (mPa s)	Time at which complex viscosity reaches 1 Pa.s (min)	Time to gelation (min) (σ = standard deviation)
1	44	27	56 (σ = 0.2)
2	36	26	62 (σ = 0.7)
3	58	26	73 (σ = 0.4)

The data shown in Fig. 2. and Table 3 demonstrate that the anhydride structure does influence the rheological behaviour of the resin in the later stages of the reaction. Blends **1** and **2**, containing the more structurally similar anhydrides (varying only in the degree of unsaturation), display very similar profiles of complex viscosity throughout the reaction, but the influence of methyl-3,6-endomethylene-1,2,3,6-tetrahydrophthalic (MHAC-P) anhydride is more profound. This is highlighted in the difference in gel times, which in these instances was determined from the cross over in storage and loss moduli. The time to gelation is much longer for resin **3** (containing methyl-3,6-endomethylene-1,2,3,6-tetrahydrophthalic anhydride) taking some 73 minutes to gel, compared with 56 minutes for the blend **1** (containing 3- or 4-methyl-1,2,3,6-tetrahydrophthalic anhydride). This is probably due to the MHAC-P anhydride having a more sterically hindered structure than the other anhydrides, leading to a delay in the propagation and the development of viscosity as the reaction processed.

3.3 Examining the thermal polymerisation of the blends.

Of equal importance to the rheological properties is the knowledge of the reactivity of the resin and characterisation of its thermal properties, DSC was used to determine this both qualitatively and quantitatively (*i.e.* the relationship between the anhydride structure and the effect of this upon the onset of reaction, exothermic peak (the temperature at which the exothermic rate is maximal) and the enthalpy of reaction). The DSC thermograms of the uncured resins are given in duplicate for each of the three blends (Fig. 3), where the hatched line represents one repeat run, which shows the precision of the data.

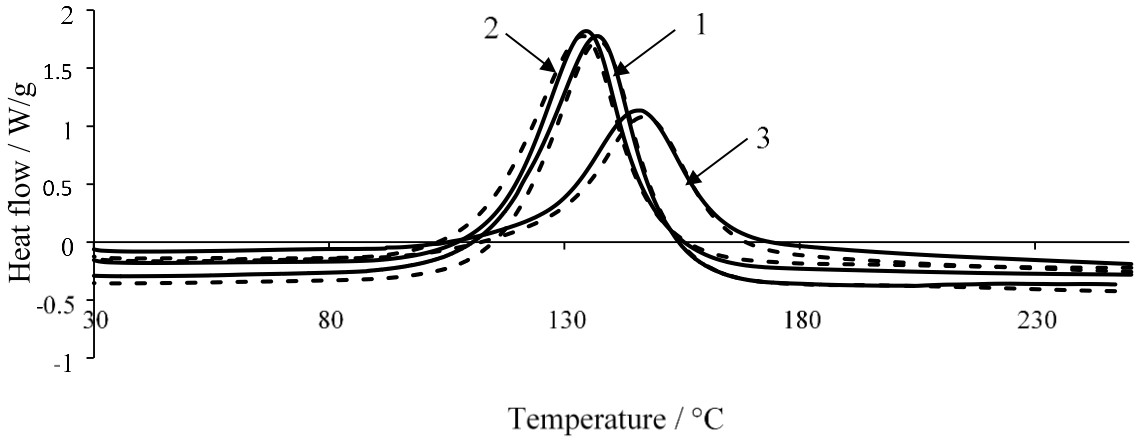

Figure 3. DSC thermograms of the three resin blends.

DSC data obtained from dynamic experiments conducted at 10 °C/min are presented in Table 4, for both uncured resin and the cured resin. The data presented (averaged values from three DSC thermograms) all showed typical standard deviations (σ): σ = 1 for T_0 and $T_{exo,}$ and T_g; and σ = 7 for reaction enthalpy (ΔH_c). Resin blends **1** and **2** yield very similar temperatures for the onset of polymerisation and exothermic peak maxima, with the less reactive blend **3** showing a more delayed thermal event in a higher temperature regime (*e.g.* peak maximum some 10 °C higher).

Table 4. Dynamic DSC data for resin blends **1**, **2**, and **3**, ramp rate 10 °C/min.

Blend	T_o (°C)	T_{exo} (°C)	ΔH_c		$T_{g(ult)}$ (°C)
			(J/g)	(kJ/mol)	
1	115	137	327	105	100
2	109	133	301	97	107
3	122	147	242	78	117

Key: T_o = Temperature of onset of polymerization, T_{exo} = Exothermic peak temperature, ΔH_c = reaction enthalpy.

Using MDSC thermograms, the degree of cure (α) was calculated for all blends, which had been cured using the same prescribed oven cure cycle, using Equation 1, and the data given in Table 5.

$$\alpha = 1 - \frac{\Delta H_{pc}}{\Delta H_c} \qquad \text{Eq. 1}$$

where ΔH_c is the reaction enthalpy (Table 4), ΔH_{pc} is the residual cure, and α is the degree of cure.

Table 5. MDSC data for the oven cured resin blends **1**, **2**, and **3**.

Blend	ΔH_{pc} (J/g)	α	T_g (°C)
1	37	0.89	102
2	38	0.88	103
3	48	0.83	100

From the MDSC thermograms the residual cure is approximately equal for blends **1** and **2** at 89% and 88% respectively, with blend **3** having a lower degree of cure at 83%. There is a difference in the T_g observed from the rescan of the resin cured in the DSC ($T_{g(ult)}$), Table 4, which is ostensibly fully cured, since no measurable residual cure was observed, and the T_g observed from the MDSC, Table 5, of a resin sample cured following the prescribed oven cure cycle. The lower T_g is recorded from the MDSC due to the lower conversion achieved with the prescribed oven cure cycle. The T_g for blend **3** deviated most for samples cured in the oven and the calorimeter as the lowest conversion of 0.83 is achieved *via* the oven cure cycle.

3.5 Kinetic analysis of the thermal polymerisation of the binary blends.

In order to determine the kinetics of the polymerization reaction, a variety of dynamic heating experiments were conducted using DSC for each blend at heating rates of 3, 5, 10, 15, and 20 °C/min (Fig. 4). As expected, the effect of increasing the heating rate is to shift the value of T_{exo}

to a higher temperature regime in all three blends. Assuming first order reaction kinetics, the Kissinger and Ozawa methods can be used to yield a preliminary assessment of the reaction kinetics in each of the three blends [19-21].

Using the Kissinger method, Equation 2, the activation energy, E_a and the pre-exponential factor, A, were determined for each of the three blends:

$$\ln\left(\frac{\beta}{{T_{max}}^2}\right) = ln\left(\frac{AR}{E_a}\right) - \frac{E_a}{RT} \qquad \text{Eq. 2}$$

where, β is the heating rate, T_{max} is the exothermic peak maximum (in Kelvin), E_a is the activation energy, which is the energy barrier which the reaction must overcome for the reaction to proceed, A is the pre-exponential factor, which is interpreted as the probability that a molecule will have energy E_a and participate in the reaction, R is the gas constant (8.314 J/K/mol).

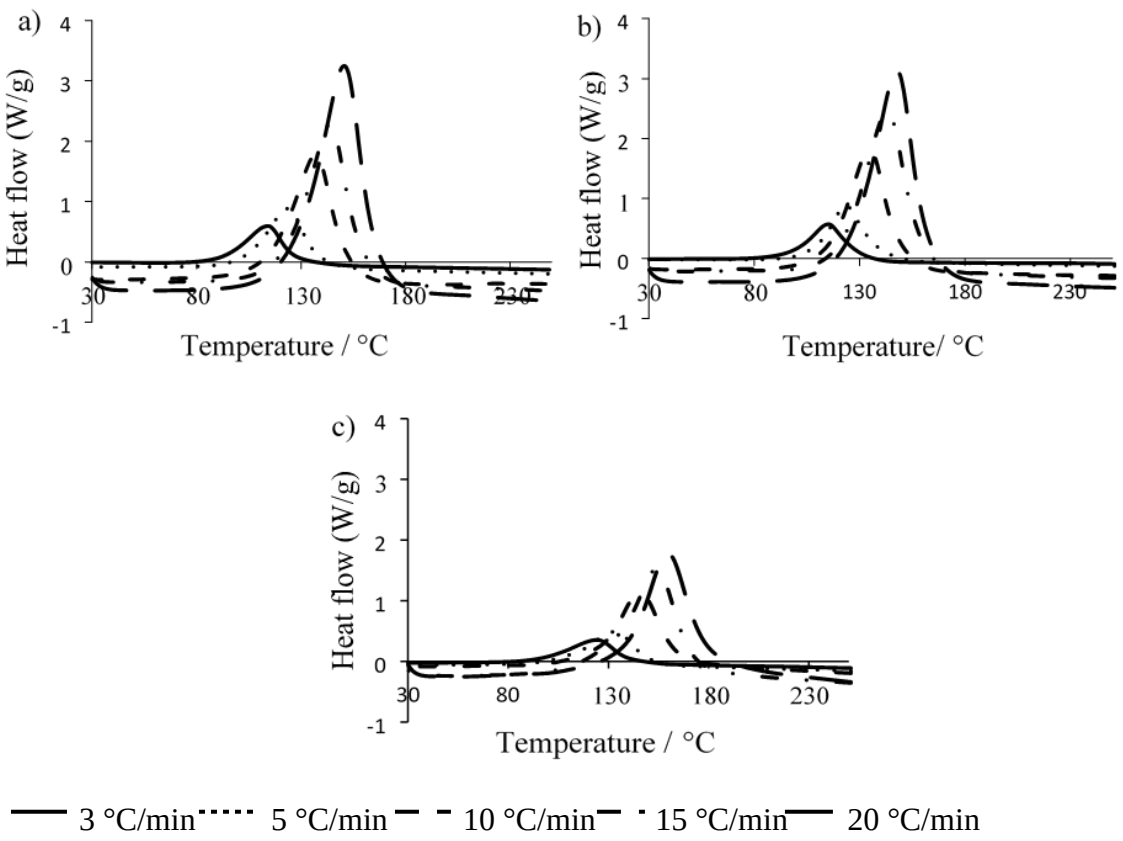

Figure 4. DSC thermograms of selected compounds: **1** (a), **2** (b), and **3** (c) at several different heating rates: 3, 5, 10, 15, 20 °C/min.

By plotting a graph of $\ln\beta = (T_{max})^2$ *versus* $1/T_{max}$, the activation energy E_a and pre-exponential factor can be determined from the gradient and y-intercept respectively. A complementary method was proposed by Ozawa, and this considers the effect of heating rate and uses the inverse of the exothermic peak maximum and the logarithm of the heating rate, thus allowing the E_a to be determined using Equation 3.

$$ln\beta = const - 1.052\frac{E_a/_R}{T_{max}} \qquad \text{Eq. 3}$$

The plots of the kinetic data obtained using both the Kissinger and Ozawa methods are presented for each of the blends **1** (Fig. 5 a), **2** (Fig. 5 b), and **3** (Fig. 5 c). Using the aforementioned equations, the E_a was determined from the gradient of the lines, in all cases the correlation coefficient ($R^2 > 0.99$) confirms that the models are valid.

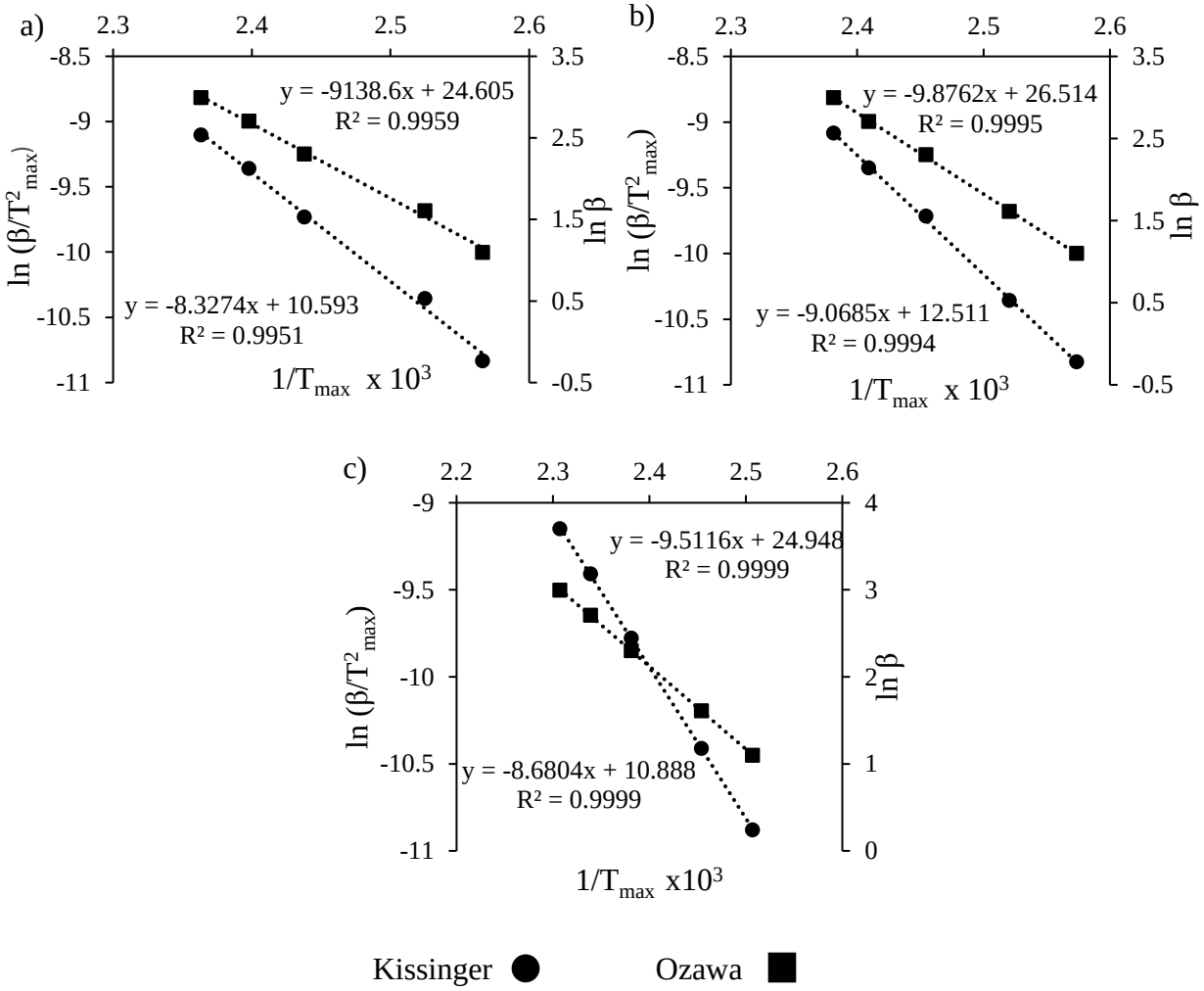

Figure 5. Kissinger and Ozawa plots of the three resin blends **1** (a), **2** (b), and **3** (c).

The Kissinger method also enables the pre-exponential factor (*A*) to be determined and therefore the rate constant (*k*) for the reaction can be calculated using the Arrhenius equation as given in Equation 4.

$$k = Ae^{\left(\frac{-E_a}{RT}\right)} \quad \text{Eq. 4}$$

where, k is the rate constant and T is the temperature. To compare the rate constants the cure temperature (348 K (75 °C)) was chosen. The values calculated are given in Table 6.

Table 6. Kissinger and Ozawa kinetic analysis for the three blends.

Blend	Ozawa method E_a (kJ/mol)	Kissinger method E_a (kJ/mol)	Pre-exponential factor, A (s^{-1})	Rate constant (10^{-3} k) at 348 K (s^{-1})
1	72.2	69.2	3.3×10^8	14.0
2	78.1	75.4	2.5×10^9	12.0
3	75.2	72.2	4.6×10^8	6.8

Interestingly, the reduced reactivity of blend **3** is shown in the lowest first order rate constant ($k = 6.8 \times 10^{-3}$ s^{-1} at 348 K), while the activation energy is found to be highest for blend **2**. Similarly, of the three blends, **1** displays the fewest collisions ($A = 3.3 \times 10^8$ s^{-1}), so the reason for the disparity is more complex [22].

In 2012, a study on the cure kinetics of an amine-cured bisphenol-A epoxy derivative resin for wind turbine blade applications was conducted by Hardis [23] using Kissinger analysis and found the E_a to be 52.37 kJ/mol and A to be 1.66×10^{15} s^{-1}. A more closely-related study by Yu *et al.* [24] used a bisphenol-A type epoxy with an anhydride curing agent and diluent and reported an apparent E_a of 73.87 kJ/mol and $A = 4.4 \times 10^7$ min^{-1}, thus showing comparable results to those obtained in the present study.

3.4 DMA data

Storage modulus and loss factor are shown as a function of temperature for the three resin blends (Fig. 6), from which it is apparent that the storage moduli, below T_g, are very similar for all three resin blends, at 3.5 GPa (Fig. 6(a)). In this work the T_g (as measured by DMA, Fig. 6(b) is reported as the loss factor peak in the tan delta response (ratio between storage and loss modulus): all three blends display similar values (**1** - 97 °C, **2** - 98 °C, and **3** - 95°C). The difference in the response of the three blends is apparent in the magnitude of the rubbery modulus, Fig 6(a), with resin blend **1** showing the most rigid behaviour above T_g. Fig 6(b) shows that blends **2** and **3** (more so) exhibit a secondary peak at approximately 130 °C. This behaviour is likely due to the resin post-curing at these higher temperatures. It has already been established that resin blends **2** and **3** achieve lower conversions at the prescribed cure cycle, with **3** showing lowest conversion due to steric effects. The higher temperatures to which the sample is exposed to suing DMA testing could enable post-cure and thus this secondary peak is observed as the resin cures further.

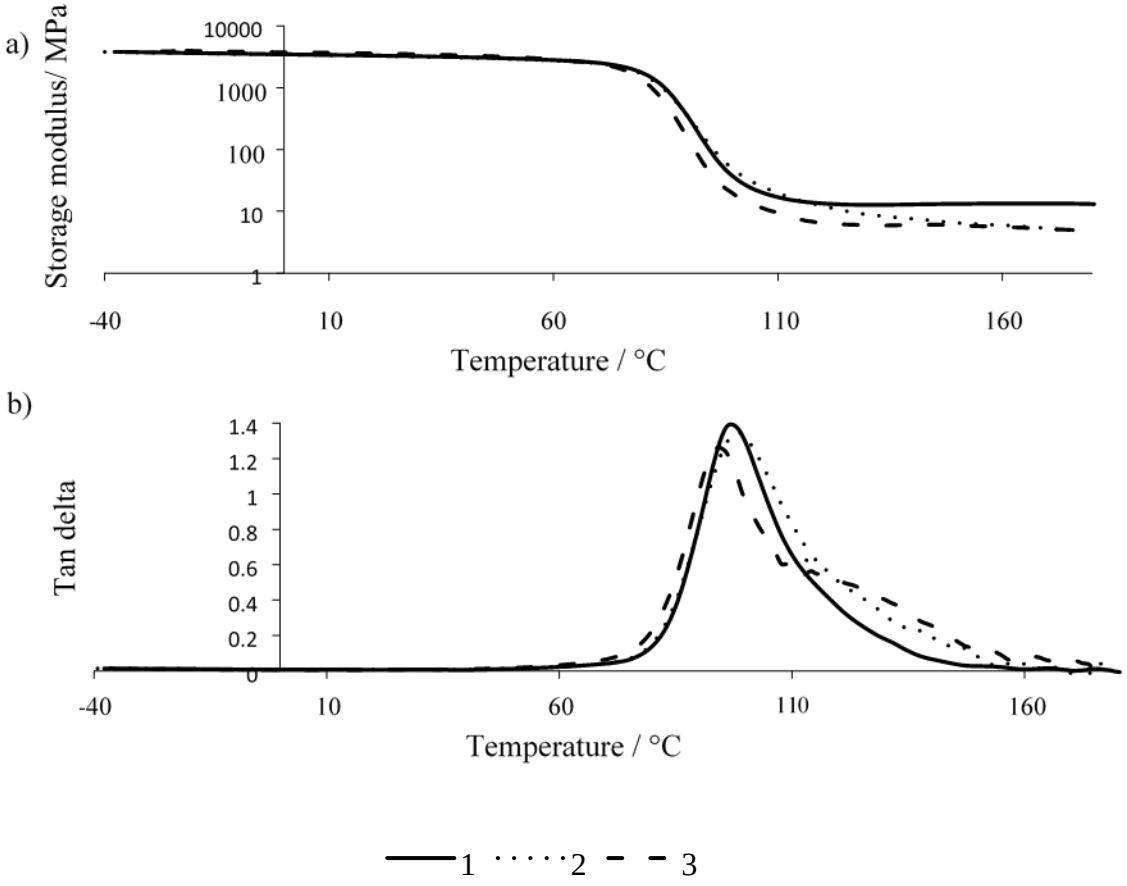

Figure 6. (a) storage modulus and (b) loss factor data (shown as tan delta) for the three cured resin blends **1**, **2**, and **3**.

The crosslink density of a lightly crosslinked material can be determined using Equation 5 from the statistical theory of rubber elasticity. Ishida and Allen [25], and Hamerton *et al.* [26] successfully used this equation to assess qualitatively the crosslink density of polybenzoxazines, which works well for homologous series, and a similar approach was adopted herein.

$$G' = \phi \nu R T_e \qquad \text{Eq. 5}$$

where, G' is the storage modulus in the rubber region (T_e), ϕ is the front factor which is unity for ideal rubbers, R is the gas constant (8.314 J/K/mol) and T_e is the absolute temperature (T_g + 50 °C) and ν is the crosslink density of the material.

Using the same relationship, the crosslink density of the cured epoxy resin blends was calculated and are compared in Table 7. From this initial assessment it is apparent that blend **1** represents the most highly crosslinked network, while blends **2** and **3** are practically the same.

Table 7. Crosslink densities for the anhydride-cured epoxy blends.

Blend	T_g (K)	T_e (K)	G' at T_e (MPa)	ν (x10^3 mol/cm^3)
1	370	420	11.9	3.42
2	371	421	8.0	2.30
3	368	418	8.2	2.37

3.5 Examination of network formation using FTIR spectroscopy.

Infrared spectroscopy was conducted on the uncured resin and a cured resin plaque. As the contact with the crystal is much poorer for the cured resin, the amplitude of the peaks cannot be used to accurately determine the degree of cure. However, the frequency of the vibrations can be used to infer which bonds are present in the sample and therefore it can be used to gain information regarding the reaction mechanism. As the reaction mechanism is the same for all three blends, only the data from resin blend **1** will be reported for clarity. The FTIR spectra for resin blend **1** in both its uncured and cured state are given in Fig. 7. For uncured resin blends the main peaks of interest were those at 1775 cm^{-1} and 915 cm^{-1} which correspond to bond frequencies of the carbonyl bond of the anhydride ring and the epoxide ring respectively. In the cured resin spectra these bonds are either not present or significantly reduced and there is a new peak at 1732 cm^{-1}. This peak corresponds to the alkanoate ester, formed following the epoxide ring opening *via* the reaction of

the epoxy with the anion formed from the pre-reaction of the anhydride and the tertiary amine (Figure 1).

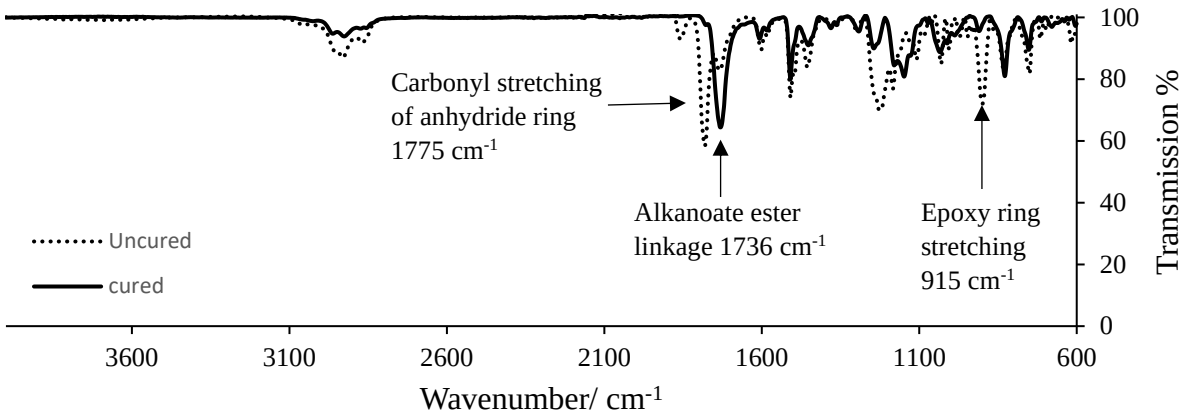

Figure 7. FTIR transmission spectra for resin blend **1**.

3.6 Thermal stability of the cured resin blends.

Simultaneous thermal analysis (STA) was employed to examine the thermal stability of the three cured resin blends employing the different anhydrides (Fig. 8).

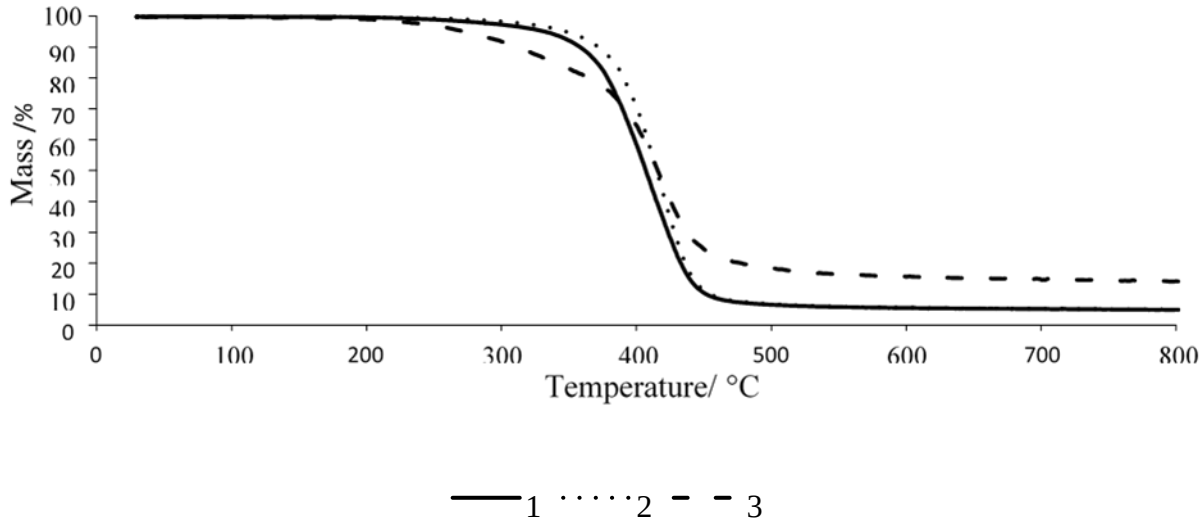

Figure 8. Thermogravimetric analysis (TGA) data for the three cured resin blends **1**, **2**, and **3**.

A more detailed set of data (Table 8), gives the temperature for the onset of degradation, mass loss, and residual char yield for each of the three cured blends. The cured resins show distinctly different behaviour: cured blends of **1** and **2** undergo the onset of degradation at similar temperatures but blend **1** displays poorer thermal stability over the temperature range (350 to 425 °C), relating to the breakdown of aromatic rings. Beyond this point both cured blends of **1** and **2** display identical char yields (5%), despite the disparity in the crosslink densities. Most notable is the behaviour of the cured blend **3**, which displays the poorest initial thermal stability (relating to the breakdown of single bonds), but soon becomes the most stable of the resins above 400 °C, yielding the highest char yield (14% at 800 °C) [21,22].

Table 8. Thermal stability data for the anhydride-cured epoxy blends.

Blend	Temperature (°C) at which % mass lost				Y_c (%)
	$T_{5\%}$	$T_{10\%}$	$T_{20\%}$	$T_{40\%}$	
1	328	356	377	398	5
2	348	372	390	408	5
3	273	310	365	405	14

Key: $T_{x\%}$ = temperature (°C) at which % mass is lost, Y_c = char yield remaining at 800 °C.

Although onset of large mass loss for resin blend **3** occurs at 372 °C it can be seen (Fig. 8) that a smaller mass is lost prior to this point with the process commencing at around 200 °C. It is proposed that at this temperature a pericyclic retro-Diels-Alder reaction occurs in the norobornene moiety of anhydride D, leading to the elimination of a methylated cyclopentadiene species from the resin [27,28], which would correspond to the initial mass loss before proceeding to degrade in a similar manner to the other resin blends. Similar mechanisms form the basis for the cure of the commercial polyimide PMR-15, where under the specified processing conditions (sealed system

and under pressure), the cyclopentadiene participates in the crosslinking of the corresponding bismaleimide [29]. Resin blend **3** also has a much higher char yield than the other resin blends, and it is assumed this is due to the different ratios of sp^3:sp^2 carbons, as it is well known in literature that high aromaticity and cyclic structures lead to higher char yields [30].

4. Conclusions

The cure of a commercial difunctional epoxy resin has been studied in the presence of three acid anhydrides, differing in the nature of the cycloaliphatic moiety. Data from rheological and thermal analyses confirm that all three anhydrides form suitable blends for infusion, each displaying low viscosity and favourable cure kinetics at moderate temperatures. Anhydrides with similar chemical structures (*i.e.* **1** and **2**) yield cured blends with similar dynamic mechanical properties (*i.e.* modulus and T_g) and thermal stability. The inclusion of norbornene moiety in blend **3** raises the viscosity of the blend significantly and leads to a slower reaction and marginally lower conversion, despite displaying a similar activation energy and collision factor to the other blends. The resulting cured polymer blend for this anhydride displays lower thermal stability (postulated as being due to a retro-Diels-Alder mechanism), but a higher char yield when compared to the other cured blends. This work is currently addressing the influence of the curing agent structure on the interfacial and mechanical properties of the resulting glass and carbon fibre reinforced laminates and these will be reported in a future publication.

AUTHOR INFORMATION

Author Contributions

The manuscript was written through contributions of all authors. All authors have approved the final version of the manuscript.

Funding Sources

The work of BR was supported by the Engineering and Physical Sciences Research Council (EPSRC) through the EPSRC Centre for Doctoral Training in Advanced Composites for Innovation and Science [grant number EP/L016028/1], the EPSRC Future Composites Manufacturing Hub [grant number EP/P006701/1], and a studentship from Hitachi Chemical Co. Ltd. [contract number 66850].

Acknowledgments

We thank Hitachi Chemical Co. Ltd. for the supply of the materials studied in this programme.

Abbreviations

DGEBA, diglycidyl ether of bisphenol A; (M)DSC, (modulated) differential scanning calorimetry; T_g, glass transition temperature; DMA, dynamic mechanical analysis; FTIR Fourier transform infrared spectroscopy; STA, simultaneous thermal analysis; TGA thermal gravimetric analysis; VaRTM, vacuum assisted resin transform moulding.

References

[1] L. Mishnaevsky Jr, Composite Materials in Wind Energy Technology, Thermal to mechical energy conversion: Engines and reqirements, Encyclopedia of Life Support Systems (EOLSS)., UNESCO, Eolss Publishers, Oxford. (2011)

[2] Meet the Haliade-X, the World's Most Powerful and Efficent Offshore Wind Turbine- GE Renewable Energy, (2019). https://www.ge.com/renewableenergy/stories/new-wind-turbine-to-increase-efficiency-in-offshore-wind-farms (accessed June 24, 2019).

[3] F.M. Jensen, K. Branner, Chapter 1: Introduction to wind turbine blade design, in: P. Brondsted, R.P. Nijssen (Eds.), Advances in Wind Turbine Blade Design and Materials, Woodhead Publishing Limited, (2013): pp. 3–25.

[4] P.S. Veers, T.D. Ashwill, H.J. Sutherland, D.L. Laird, D.W. Lobitz, D.A Griffin, J.F. Mandell, W.D. Musial, K. Jackson, M. Zuteck, A. Miravete, S.W. Tsai, J.L. Richmond, Trends in the design, manufacture, and evaluation of wind turbine blades, Wind Energy. 6 (2003) pp. 245–259.

[5] P. Brondsted, R.P. Nijssen, Chapter 6: Fatigue as a design driver for composite wind turbine blades, in: Advances in Wind Turbine Blade Design and Materials, Woodhead Publishing Limited, (2013): pp. 175–209.

[6] J.D.H. Hughes, The Carbon Fibre / Epoxy Interface - A Review, Compos. Sci. Technol. 41 (1991) pp. 13–45.

[7] C. Ng, L. Ran,(Eds.), Offshore Wind Farms: Technologies, Design and Operation, Woodhead Publishing Limited, (2016)

[8] C. May (Ed.), Epoxy Resins: Chemistry and Technology, 2nd ed., CRC Press, New York, USA, (1987).

[9] B. Ellis (Ed.), Chemistry and Technology of Epoxy Resins, Springer, Dordrecht (1993).

[10] F.C. Binks, G. Cavalli, M. Henningsen, B.J. Howlin, I. Hamerton, Investigating the mechanism through which ionic liquids initiate the polymerisation of epoxy resins, Polymer. 139, (2018) pp. 163–176.

[11] M.K. Antoon, J.L. Koenig, Crosslinking mechanism of an anhydride-cured epoxy resin as studied by fourier transform infrared spectroscopy., J. Polym. Sci. A1. 19, (1981) pp. 549–570.

[12] W.H. Park, J.K. Lee, K.J. Kwon, Cure behavior of an epoxy-anhydride-imidazole system, Polym. J. 28 (1996) pp. 407–411.

[13] L. Nunez, F. Fraga, L. Fraga, T. Salgado, J.R. Anon, Determination of the optimum epoxy/curing agent ratio: A study of different kinetic parameters, Pure Appl. Chem. 67 (2007) pp. 1091–1094.

[14] C.R. Palmese, Effect of epoxy-amine stoichiometry on cured resin material properties, J. Appl. Polym. Sci. (1971) pp. 1863–1873.

[15] P. Guerrero, K. De La Caba, A. Valea, M.A. Corcuera, I. Mondragon, Influence of cure schedule and stoichiometry on the dynamic mechanical behaviour of tetrafunctional epoxy resins cured with anhydrides, Polymer, 37 (1996) pp. 2195–2200.

[16] P.S. Rhodes, Advances in anhydride epoxy systems,in: 23rd Int. SAMPE Tech. Conf, New York, USA (1991).

[17] C. Li, K. Potter, M.R. Wisnom, G. Stringer, In-situ measurement of chemical shrinkage of MY750 epoxy resin by a novel gravimetric method, Compos. Sci. Technol. 64 (2004) pp. 55–64.

[18] B.K. Russell, C. Ward, S. Takeda, I. Hamerton, Initial studies to characterise a polymer matrix for use in composite wind turbine blades, in: ICCM21 – 21st Int. Conf. Compos. Mater. Xi'an, China (2017).

[19] H.E. Kissinger, Variation of peak temperature with heating rate in differential thermal analysis, J. Res. Natl. Bur. Stand, 57 (1956) pp. 217-221.

[20] T. Ozawa, Kinetic analysis of derivative curves in thermal analysis, Journal of Thermal Analysis, 2, (1970) pp. 301–324.

[21] J. Rocks, Characterization of Novel Co-Anhydride Cured Epoxy Resins, PhD Thesis, Queensland University of Technology, (2004).

[22] J. Barton, The application of differential scanning calorimetry (DSC) to the study of epoxy resin curing reactions, in: Epoxy Resins and Composites I. Advances in Polymer Science, vol 72, Springer, Berlin, Heidelberg, (1985) pp. 111–154.

[23] R. Hardis, Cure Kinetics Characterization and Monitoring of an Epoxy Resin for Thick Composite Structures, Graduate Thesis, Iowa State University, USA, (2012).

[24] J. Ding, W. Peng, T. Luo, H. Yu, Study on the curing reaction kinetics of a novel epoxy system, RSC Adv. 7 (2017) pp. 6981–6987.

[25] H. Ishida, D.J. Allen, Mechanical characterization of copolymers based on benzoxazine and epoxy, Polymer, 37 (1996) pp. 4487–4495.

[26] I. Hamerton, L.T. Mcnamara, B.J. Howlin, P.A. Smith, P. Cross, S. Ward, Examining the initiation of the polymerization mechanism and network development in aromatic polybenzoxazines, Macromolecules. 26 (2013).

[27] D. Birney, T.K. Lim, H.P. Koh, B.R. Pool, J.M. White, Structural investigations into the retro-Diels-Alder reaction: experimental and theoretical Studies, J. Am. Chem.Soc. 124 (2002) pp. 5091–5099.

[28] Z. Cai, B. Shen, W. Liu, Z. Xin, H. Ling, Liquid-phase cracking of dicyclopentadiene by reactive distillation, Energy Fuels. (2009) pp. 4077–4081.

[29] C. Conreur, J. Francillette, F. Lauprete, Synthesis and processing of model compound of PMR-15 resin, J. Polym. Sci. Part A Polym. Chem. 35 (2000).

[30] C.S. Chen, B.J. Bulkin, E.M. Pearce, New epoxy resins.II. The preparation, characterization, and curing of epoxy resins and their copolymers, J. Appl. Polym. Sci. 27 (1982) pp. 3289–3312.